

## **Influence of wave approach angle on square tlp's behavior in random sea**

\* Ashraf M. Abou-Rayan<sup>1)</sup> and Osama S. Hussein<sup>2)</sup>

<sup>1)</sup> *Civil Engineering Dept., Benha University., Egypt*

<sup>2)</sup> *Civil Engineering Dept., Al-Azhar University., Egypt.*

### **Abstract**

Tension leg platform (TLP) is a suitable type for very deep-water oil production. The TLP is a compliant structure behaving like a floating one. It can be modeled as a rigid body with six degrees of freedom (6-DOF), which can be conveniently divided into two categories, those controlled by the stiffness of tethers, and those controlled by the buoyancy. The former category includes motion in the vertical plane and consists of heave, roll and pitch (stiff DOF); whereas the latter comprises the horizontal motions of surge, sway and yaw (flexible DOF). This paper investigates the nonlinear response of the Square TLP configuration under different random wave approach angles,  $0^\circ$  and  $30^\circ$ . Random waves were generated according to Pierson-Moskowitz spectrum and acts on the structure in the surge direction. The hydrodynamic forces evaluation is based on the modified Morison equation. Coupling effect and added mass are considered in the developing of the equation of motion. The nonlinear equation of motion is solved in the time domain utilizing the modified Euler scheme. Time history responses, phase planes, and Power spectrum densities (PSD) for the nonlinear responses for both approach angles are shown. It was found that, Variation of wave approach angle activates specific degrees of freedom like sway and roll which otherwise are not activated under unidirectional wave force.

**Keywords:** Compliant offshore structures; Random sea wave forces, Nonlinear response.

### **1. Introduction**

TLP's are floating flexible (compliant) structures with six degrees of freedom; (surge, sway, heave, roll, pitch, and yaw) see fig. 1. They undergo relatively long period of vibration associated with the motion in the horizontal plan. The inherited large deformations in their horizontal plan, causes nonlinearity in the structure stiffness matrix. A number of studies have been conducted on the dynamic behavior of TLP's under both regular and random waves. The literature on offshore structures is huge. We will only highlight few papers which are relevant to the present work. Tabeshpour et al. (2006), have investigated the dynamic responses of a square TLP configuration under unidirectional random waves. They considered a  $30^\circ$  approach angle for the wave. A beating phenomenon was clear in roll and pitch accelerations. Chandrasekaran et al.

(2007) focused on the response analysis of triangular tension leg platform for different wave approach angles and studied its influence on the coupled dynamic response of triangular TLP's. They concluded that, the variation of wave approach angle activates some degrees of freedom that were not activated by unidirectional wave. TLPs. Kurian et al. [2008a] developed a numerical study on the dynamic response of square TLPs subjected to regular and random waves. They also conducted parametric studies with varying parameters such as water depth, pretension, wave angle and position of center of gravity. Kurian et al. (2008b) developed a numerical study on determining the dynamic responses of square and triangular TLPs subjected to random waves. They found that the responses of triangular TLPs are much higher than those of square TLP. Low (2009) presented a formulation for the linearization of the tendon restoring forces of a TLP. He found that, the linearization technique facilitates accurate predictions of the mean offsets and the response variances, including the slow-drift component. Also, Abdel-Rahman et al. [2012], have studied the nonlinear analysis of offshore structure under wave loading. Abou-Rayyan et al. (2012) have investigated the dynamic responses for a square TLP configuration under uni-directional regular waves in the surge direction of the platform. They also have considered the coupling effect between all six degrees of freedom. The analysis was carried out using modified Morison equation in the time domain with water particle kinematics using Airy's linear wave theory. The influence of nonlinearities due to hydrodynamic forces and the coupling effect between surge, sway, heave, roll, pitch and yaw degrees of freedom on the dynamic behavior of TLP's was investigated. The stiffness of the TLP was derived from a combination of hydrostatic restoring forces and restoring forces due to cables and the nonlinear equations of motion were solved utilizing Newmark's beta integration scheme. The effect of wave characteristics such as wave period and wave height on the response of TLP's was evaluated. Only uni-directional waves in the surge direction was considered in the analysis. They found that, the coupling has no effect on the surge or the heave responses and has insignificant effect on the pitch response. Also, from the phase plane responses they concluded that, that the steady state behavior of the TLP is periodic and stable. Murray Rudman, n, Paul W. Cleary (2013), have studied the interaction of a rogue wave on a TLP yields complex platform dynamics that has been predicted using the Smoothed Particle Hydrodynamics (SPH) technique. A particle resolution study showed that at a resolution of 1.5 m, the key impact phenomena were very similar to those predicted at a higher (1.0 m) resolution. Although the results are not fully numerically converged at 1.5 m, the differences are very small and justify the use of this particle resolution. Liu, Yuanchuan and Wan, Decheng (2013), performed a series of numerical simulation on the interaction of a triple-hulled offshore observation platform with different incident waves. All of the simulations are implemented utilizing the open source tools of OpenFOAM. Duration curves of motion characteristics and loads acting on the platform are obtained, and a comparison between the results of the amplitude in different incident waves is obtained. PeiWen, et al. [2014], have studied the effect of pontoons on the free surface elevation and near-trapping phenomenon of a TLP., They concluded that: 1) The effect of pontoons on the diffracted wave field in the vicinity of the structures is found to be dependent on the incident wave length. For short incident waves, pontoons are found to have a weak effect on the diffracted wave field. In contrast, pontoons have an appreciable effect on the magnitude of the free surface

elevation for long incident regular waves. 2) Numerical results show that near-trapping phenomenon can occur inside a TLP platform and it plays a strong role not only for the first-order free surface elevation but also for the second-order free surface elevation. 3) At the second-order near-trapping frequency, pontoons increase the largest response notably.

Recently Abou-Rayan and Hussein (2014), developed a numerical scheme to investigate the nonlinear dynamic response characteristics of a square TLP configuration under random waves. The time history of randomwave is generated based on Pierson-Moskowitz spectrum and acts on the structure in the surge direction. The hydrodynamic forces are calculated using the modified Morison equation according to Airy's linear wave theory. Utilizing modified Euler equation step-by-step integration technique, the solution for the equation of motion was obtained. They found that the phase plane and the response spectra show a steady state behavior and the structure is quasi-periodic and stable. Also, for the orientation of the TLP and for the unidirectional wave considered, translational (surge and heave) and rotational (pitch) degree-of-freedom (DOF) responses are influenced significantly. Variations in water particle kinematics with water depth, induced forces and moments activate in all six DOF, but the response is predominant in only three DOF.

In this investigation, a numerical scheme has been developed to investigate the nonlinear dynamic response characteristics of a square TLP configuration under random waves. Two wave approach angles are considered,  $0^\circ$  and  $30^\circ$ . The time history of randomwave is generated based on Pierson-Moskowitz spectrum and acts on the structure in the surge direction. The hydrodynamic forces are calculated using the modified Morison equation according to Airy's linear wave theory. Utilizing modified Euler equation step-by-step integration technique, the solution for the equation of motion was obtained.

## 2. Equation of Motion

The equation of motion is coupled and nonlinear and can be written as, Abou-Rayan et al. (2012):

$$[M]\{\ddot{x}(t+\Delta t)\} + [C]\{\dot{x}(t+\Delta t)\} + [K]\{x(t+\Delta t)\} = \{F(t+\Delta t)\} \quad (1)$$

Where **[M]** is the structure mass matrix; **[C]** is the structure damping matrix; **[K]** is the structure stiffness matrix; and **{F (t+Δt)}** is the hydrodynamic force vector. **x**, **ẋ**, and **ẍ** are the structural displacement vector, the structural velocity vector, and the structural acceleration vector respectively. Time history of the Randomwave is generated based on Pierson-Moskowitz spectrum. Utilizing Morison's equation and using Airy's linear wave theory, wave forces are calculated at the instantaneous equilibrium position of the TLP acting in the surge direction. Added mass coefficients in the mass matrix and coupling effect were considered in the model. Wave force coefficients,  $C_d$  (Drag coefficient= 1) and  $C_I$  (Inertia coefficient=2), are the same for the pontoons and the columns and are independent of frequencies as well as constant over the water depth.

The instantaneous total hydrodynamic force is determined at each time station with the assigned values of the structural displacements, velocities and accelerations. The wave forces are computed using the modified Morison's equation, which is:

$$F(x, y, t) = 0.5 \rho_w C_d (\dot{u} - \dot{x} + \dot{u}_c) |\dot{u} - \dot{x} + \dot{u}_c| + 0.25\pi D^2 \rho_w C_I \ddot{u} \pm 0.25\pi D^2 (C_I - 1) \rho_w \ddot{x} \quad (2)$$

Where,  $\dot{u}$  is the horizontal water particle velocity,  $\dot{u}_c$  is the current velocity,  $\ddot{u}$  is the horizontal water particle acceleration, and  $D$  is the diameter of the column. The last term of Eq. (2) is the added mass term and a positive sign is used when the water surface is below the mean sea level and the negative sign is used when the water surface is above the mean sea level. The force vector which is at an inclination angle with the surge direction ( $0^\circ$  and  $30^\circ$ ) is given by:

$$F(x, y, t) = [F_1 F_2 F_3 F_4 F_5 F_6]^T \quad (3)$$

To solve the equation of motion a step-by-step integration scheme was developed based on the modified Euler method. The analysis was carried out for dynamic response in both time and a frequency domain. The mathematical model derived in this investigation is based on the TLP model studied by Abou-Rayan et al. (2012), for detailed description of the hydrodynamic data and the geometric properties and the derivation of the equation of motion, the reader is referred to aforementioned reference.

### 3. Representation of Wave Spectra

Researchers have studying ocean waves have proposed several formulations for wave spectra dependent on a number of parameters (such as wind speed, fetch, or modal frequency). One of the simplest descriptions for the energy distribution is the Pierson-Moskowitz (P-M) spectrum. It is an empirical relationship that defines the distribution of energy with frequency within the ocean. It assumes that if the wind blows steadily for a long time over a large area, then the waves will eventually reach a point of equilibrium with the wind. This is known as a fully developed sea. Pierson and Moskowitz developed their spectrum from measurements in the North Atlantic during 1964, and presented the following relationship between energy distribution and wind.

$$S_{\eta\eta}(\omega) = \frac{H^2 T_e}{8\pi^2} \left(\frac{T_e \omega}{2\pi}\right)^{-5} \exp\left[-\frac{1}{\pi} \left(\frac{T_e \omega}{2\pi}\right)^{-4}\right] \quad (4)$$

Where  $H$  is the wave height in m,  $T_e$  is energy period in sec and  $\omega$  is the angular frequency. The normalized Pierson-Moskowitz spectrum for  $H = 15$  m and  $T_e = 15$  sec is shown in Fig. 2. Real random waves are not sinusoidal. However, they can be represented with a good approximation as superposition of regular waves. The sea surface elevation is given by:

$$\eta(x, t) = \lim_{N \rightarrow \infty} \sum_{n=1}^N A_n \cos(k_n x - \omega_n t + \alpha_n) \quad (5)$$

$$A_n = \sqrt{2S_\eta(\omega_n)\omega_0} \quad , \quad \omega_n = n\omega_0$$

Where  $A_n$  is the amplitude of the  $n$ th component wave,  $\omega_n$  is the wave frequency of the  $n$ th component wave,  $k_n$  is the wave number of the  $n$ th component wave,  $x$  is the horizontal distance from the origin,  $\alpha_n$  is the random phase angle of the  $n$ th component wave, and  $S_\eta(\omega)$  is the one-sided power spectrum for sea surface elevation. Time histories of the water particle velocity and acceleration are computed by wave superposition according to Airy's linear wave theory, utilizing the sea surface elevation time history  $\eta(x, t)$ .

Accordingly, the horizontal water particle velocity  $\dot{u}(x, t)$ , the vertical water particle velocity  $\dot{v}(x, t)$ , the horizontal water particle acceleration  $\ddot{u}(x, t)$ , and the vertical water particle acceleration  $\ddot{v}(x, t)$  are given by, respectively:

$$\dot{u}(x, t) = \sum_{n=1}^N A_n \omega_n \cos(k_n x - \omega_n t + \alpha_n) \frac{\cosh(k_n y)}{\sinh[k_n(d+\eta)]} \quad (6)$$

$$\dot{v}(x, t) = \sum_{n=1}^N A_n \omega_n \sin(k_n x - \omega_n t + \alpha_n) \frac{\sinh(k_n y)}{\sinh[k_n(d+\eta)]} \quad (7)$$

$$\ddot{u}(x, t) = \sum_{n=1}^N A_n \omega_n^2 \sin(k_n x - \omega_n t + \alpha_n) \frac{\cosh(k_n y)}{\sinh[k_n(d+\eta)]} \quad (8)$$

$$\ddot{v}(x, t) = \sum_{n=1}^N A_n \omega_n^2 \cos(k_n x - \omega_n t + \alpha_n) \frac{\sinh(k_n y)}{\sinh[k_n(d+\eta)]} \quad (9)$$

Where,  $y$  is vertical distance at which the wave kinematics is considered, and  $d$  is the water depth. A typical random sea surface elevation is shown in Fig. 3.

## 4. Results And Discussion

A numerical scheme was developed using MATLAB software where solution based modified Euler method was obtained. Wave forces ( $H = 15\text{m}$ ,  $T_e = 15\text{sec.}$ ) were taken to be acting in the direction of surge degree-of-freedom and  $30^\circ$  offset of that direction. A square ( $66\text{m} \times 66\text{m}$ ), Abou-Rayan (2012), TLP in 600 m deep water was considered for the numerical study. The geometric properties are: diameter of pontoon,  $D_p = 9\text{m}$ , diameter of columns  $D_c = 18\text{m}$ , and the tether total force = 160000 KN.

Table 1 shows the coupled natural time periods of the structure. It is observed that TLPs have very long period of vibration associated with motions in the horizontal plane (say 60 to 100 seconds). Since typical wave spectral peaks are between 6 to 15 seconds, resonant response in these degrees of freedom is unlikely to occur.

### 4.1. Surge response

The time history of the surge response for the TLPs configuration for both  $0^\circ$  and  $30^\circ$  wave approach angles are shown in Fig. 4a & b, respectively. It is clear that the maximum surge response is,  $-10\text{m} - 10\text{m}$ , for the case of wave approach angle  $0^\circ$ , where as for wave approach angle  $30^\circ$  it was reduced to  $-8\text{m} - 8\text{m}$ . Phase plane gives a

conceptual view of dynamic behavior of the structure. It is clear that the response is not a pure periodic one. The response is quasi-periodic despite the fact that the excitation is random. The Phase plan, Fig.5a &b, show that the response is oscillating between two quasi-periodic motions one is bigger than the other, relatively. In general phase plan for both wave angles of incidence, have the same oscillation patterns with the fact that one is relatively smaller,  $30^\circ$ , than the other,  $0^\circ$ . To get an insight into this behavior, the response spectra for wave height of 15 m and wave period of 15sec. was obtained for both wave angles of incidence and the results are shown in Fig. 6a &b. It is clear that we have a peak centered around a frequency of 0.2 rad/sec. That frequency is far away from the natural frequency of the square configuration, which is 0.064 rad/sec which exclude resonance phenomenon. Again, the PSD peak for wave approach angle  $30^\circ$  is less than that of wave approach angle  $0^\circ$  which is expected.

#### 4.2. Sway response

The time history of the sway response for the square TLP configuration for both  $0^\circ$  and  $30^\circ$  wave approach angles are shown in Fig. 7a &b. It is obvious that the sway maximum response is, -5m – 5m, for the case of wave approach angle  $30^\circ$ , where as for wave approach angle  $0^\circ$  it was -0.35m – 0.35m. Fig. 8a &b, show that the phase plan for both wave angles of incidence, have different oscillation patterns. Fig. 9a &b show the PSD for both waves, where the maximum peak occurs for the case of wave approach angle of  $30^\circ$ . It is clear that the wave force at approach angle of  $30^\circ$  has activated the response in that direction more than 10 times, contrary to case of  $0^\circ$ .

#### 4.3. Heave response

Fig. 10a &b show the time history of the heave response for angles of incident wave,  $0^\circ$  and  $30^\circ$ . Although there is coupling between heave degree of freedom and all other degrees of freedom, the heave response is strongly coupled with the surge degree of freedom. Hence, any offset caused in the surge degree of freedom due to wave forces will result in set-down effect in the heave direction. Accordingly, it is clear from Figs. 11 and 12, that the heave response is relatively high for wave approach angle of  $0^\circ$ . Again, from the phase plan and the PSD the response is quasi-periodic and centered around a frequency of 0.2 rad/sec. Therefore, a resonance response is unlikely to occur, since the natural frequency for that degree of freedom is 2.83 rad/sec.

#### 4.4. Pitch response

The generated wave force in the surge direction on the TLP, gives rise to a moment about the sway direction (pitch DOF). Therefore, the pitch response is directly proportional to the surge response. Figs. 13 to 15, show the time history, phase plan, and PSD, respectively. From Figures, it is clear that the maximum response occurs at  $0^\circ$  wave approach angle. Also, the response is quasi-periodic and centered around a frequency of 0.21 rad/sec excluding the resonance phenomenon.

#### 4.5. Roll response

The generated wave force in the sway direction on the TLP, gives rise to a moment about the surge direction (roll DOF). Therefore, the roll response is directly proportional to the sway response. Since the sway response for the wave approach angle  $0^\circ$  is very small, the roll response in this case is not affected (the response is in the order of  $10^{-6}$ ). On the other hand, for the case of wave approach angle  $30^\circ$  the roll response is activated with maximum response of  $-4.0 \times 10^{-4}$  to  $4.0 \times 10^{-4}$ . The roll response is not shown, since it is only activated for approach angle  $30^\circ$  with very small values..

Finally, the yaw response is not activated by any force. This indicates that this degree of freedom has not been affected by any wave direction. Therefore, the response is not shown.

## 5. Conclusions

The present study investigates the dynamic response of a square TLP under random wave forces in the surge direction and  $30^\circ$  off that direction considering all degrees of freedom of the system. A numerical scheme was developed where Morison's equation according to Airy's linear wave theory was used. Analyses were carried out in both time and frequency domains. The time history of random waves is generated based on Pierson-Moskowitz spectrum. Results for the time histories, phase plans, and power density spectrum for the affected degrees of freedom have been presented. Based on the results shown in this paper, the following conclusions can be drawn:

- 1) TLP's have very long period of vibration (60 to 100 seconds) associated with motions in the horizontal plan. Since typical wave periods are usually between 6 to 20 seconds, resonant response in these degrees of freedom is unlikely to occur.
- 2) The phase plan and the response spectra show that the steady state behavior of the structure is quasi-periodic and stable.
- 3) Variation of wave approach angle activates specific degrees of freedom like sway and roll which otherwise are not activated under unidirectional wave force, in agreement with Chandrasekaran et al. (2007) .
- 4) Surge and sway forces generated on the TLP under varied wave approach angles, also, develop moment about surge and sway directions, respectively. Hence, giving rise to pitch and roll responses.

## References

- Abdel Raheem, S.E., Abdel Aal, S.M.A., Abdel Shafy, A.G.A. and Abdel Seed, F.K. (2012), "Nonlinear analysis of offshore structures under wave loadings", Proceedings of the 15th World Conference on Earthquake Engineering 15WCEE, Lisbon, Portugal, 3270, pp.24-28.
- Abou-Rayyan, Ashraf M., and Hussein, Osama S. (2014), "Dynamic Responses of Square TLP'S to Random Wave Forces", International Journal of Civil Engineering (IJCE) Vol. 3, Issue 2, pp.103-110.

- Abou-Rayan, A.M., Seleemah, A., and El-gamal, A.R. (2012), "Response of Square Tension Leg Platforms to Hydrodynamic Forces", *Ocean Systems Engineering*, Vol.2 No.2, pp. 115 – 135.
- Chandrasekaran, S., Jain, A. K., and Gupta, A. (2007), "Influence of Wave Approach angle on TLP's Response", *Ocean Engineering*, Vol. 34, 1322–1327.
- Kurian, V.J., Gasim, M.A., Narayanan, S.P., Kalaikumar, V. [2008a], "Parametric Study of TLPs Subjected to Random Waves", ICCBT-C-19, pp.213-222.
- Kurian, V.J., Gasim, M.A., Narayanan, S.P., Kalaikumar, V. (2008b), "Response of Square and Triangular TLPs Subjected to Random Waves", ICCBT-C-12, 133-140.
- Liu, Yuanchuan and Wan, Decheng [2013], " Numerical simulation of motion response of an offshore observation platform in waves", *Journal of Marine Science and Application*, ISSN 1671-9433, 03/2013, 12, 1, pp. 89 – 97.
- Low, Y. M. (2009), "Frequency domain analysis of a tension leg platform with statistical linearization of the tendon restoring forces", *Marine Structures*, Vol. 22, 3, 480–503.
- Matlab 2012 Documentation (2012), The MathWork, Inc.
- Murray Rudman, n, Paul W. Cleary (2013), "Rogue wave impact on a tension leg platform: The effect of wave incidence angle and mooring line tension", *Ocean Engineering*, 61, pp. 123–138.
- PeiWen, CONG, Ying, GOU, and Bin, TENG (2014), "Effect of pontoons on free surface elevation around a TLP platform", *Sci China Tech Sci*, 57, pp. 163-180.
- Tabeshpour M. R., Golafshani A.A., and Seif M.S. (2006), "comprehensive study on the result of tension leg platform responses in random sea", *Journal of Zhejiang University SCIENCE A*, Vol. 7(8), 1305-1317.

Table 1. Calculated Natural Periods

<i>Flexible DOF</i>		<i>Stiff DOF</i>	
<i>Surge</i>	97.099	<i>Roll</i>	3.126
<i>Sway</i>	97.099	<i>Pitch</i>	3.126
<i>Yaw</i>	86.040	<i>Heave</i>	2.218

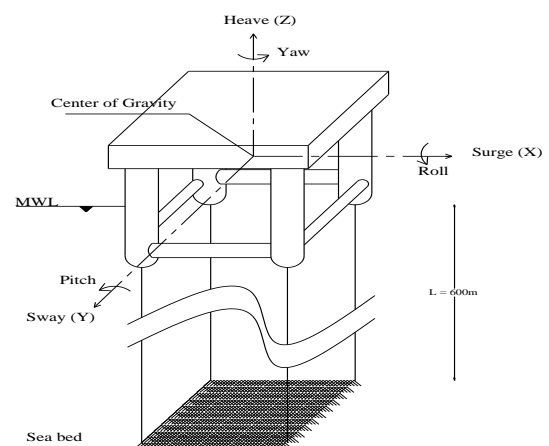
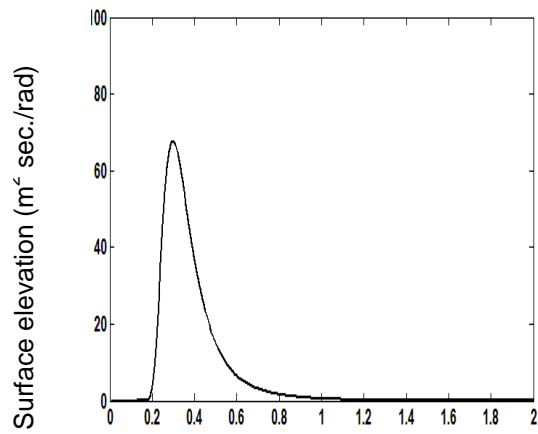


Fig. 1. : Degrees-of-freedom of the Platform





Frequency (rad/sec) Time in Sec.  
 Fig. 2: Peirson-Moskowitz PSD  
 ( $H_s = 15\text{m}$ ,  $T_s = 15\text{sec.}$ )

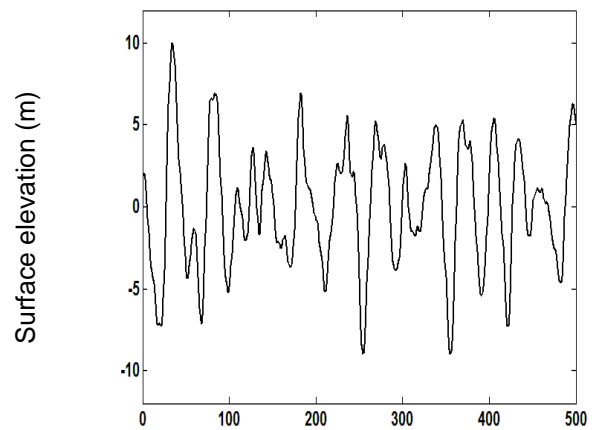


Fig. 3: Random elevation of surface wave

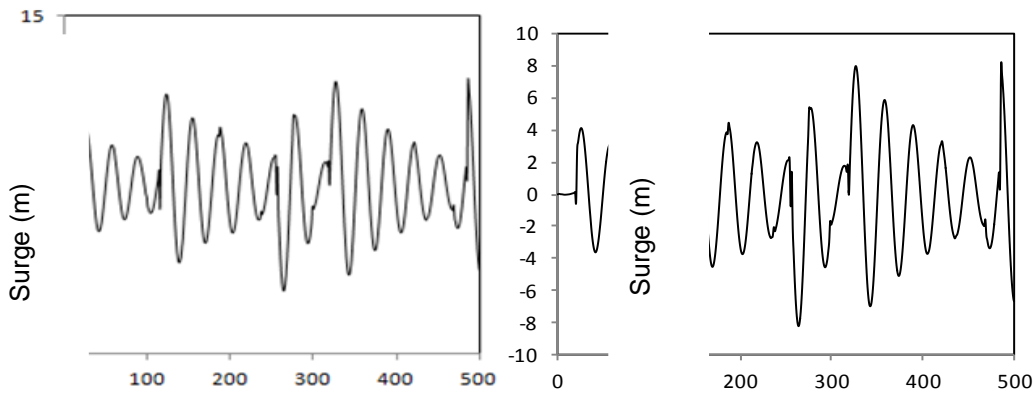


Fig. 4a: Time history of surge response ( $0^\circ$ ). Fig. 4b: Time history of surge response ( $30^\circ$ ).

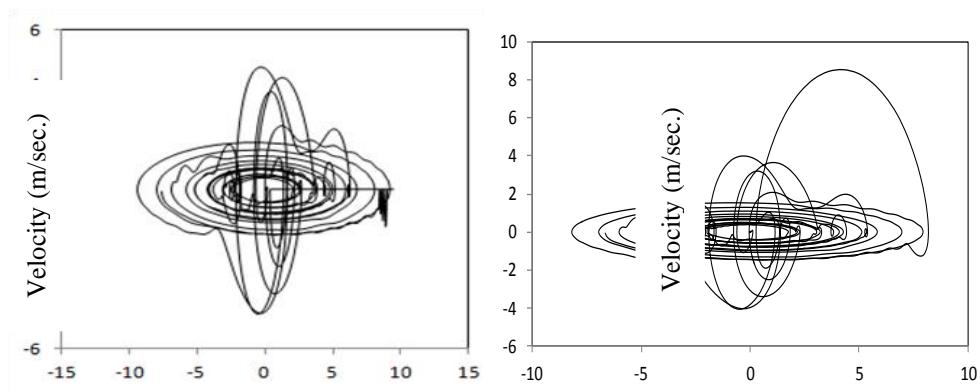


Fig. 5a: Phase plan for surge response ( $0^\circ$ ). Fig. 5b: Phase plan for surge response ( $30^\circ$ ).

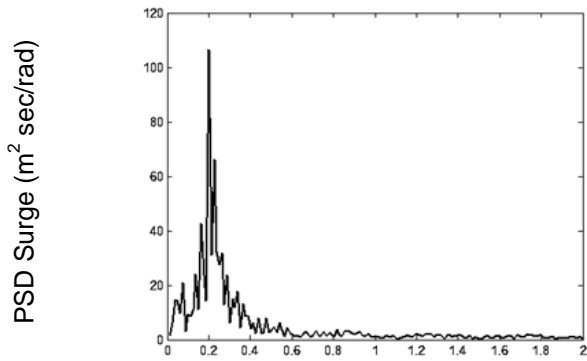


Fig. 6a: PSD of Surge displacement (0°).

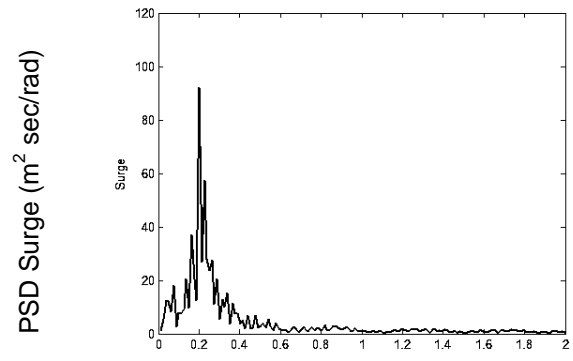
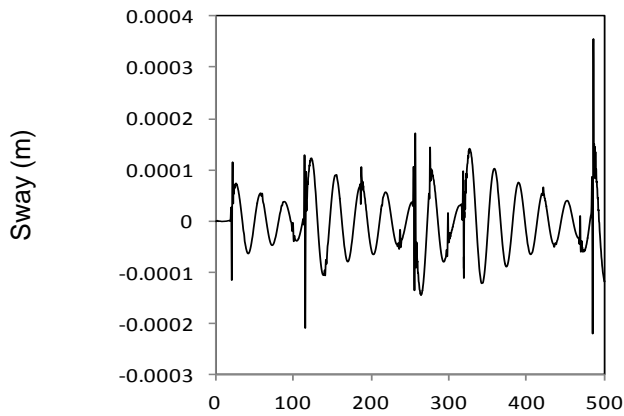


Fig.6b: PSD of Surge displacement (30°).



Time history of sway response (0°).

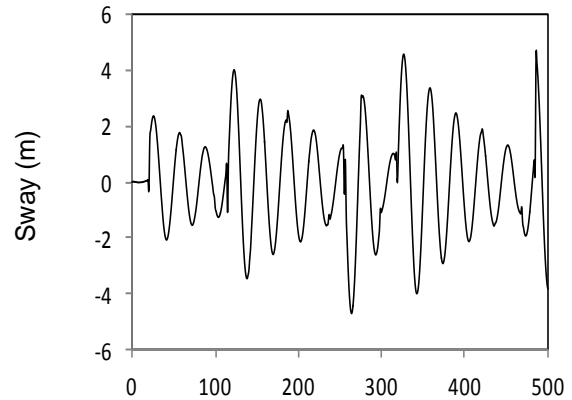


Fig. 7a:

Fig.7b: Time history of sway response (30°).

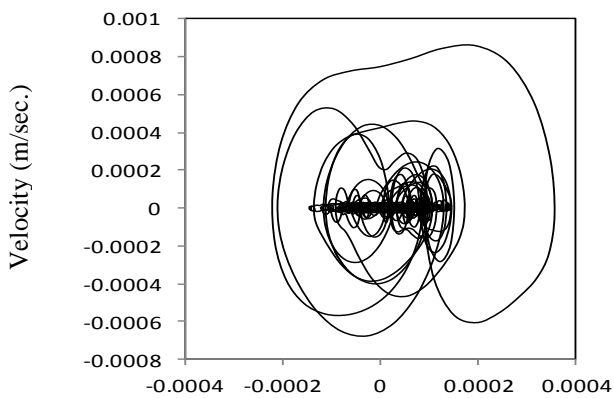


Fig. 8a: Phase plan for sway response (0°).

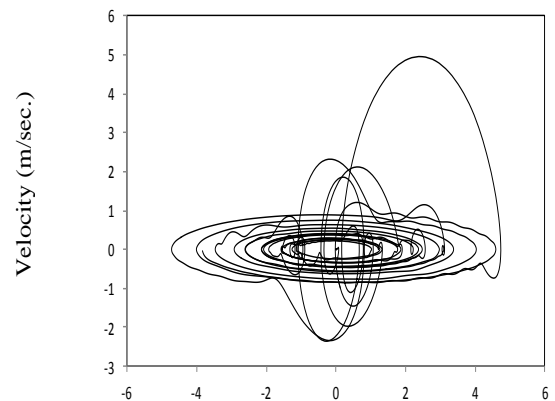


Fig.8b:Phase plan for sway response (30°).

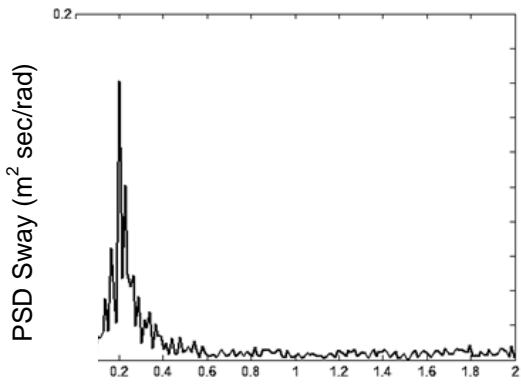


Fig. 9a: PSD of sway displacement (0°).

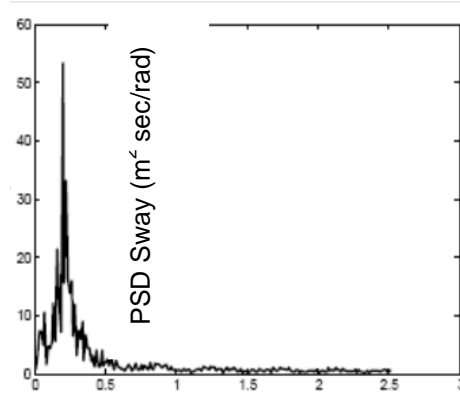


Fig.9b: PSD of sway displacement (30°).

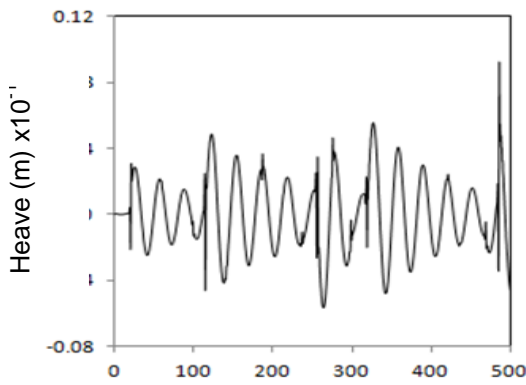


Fig. 10a: Time history of heave response (0°).

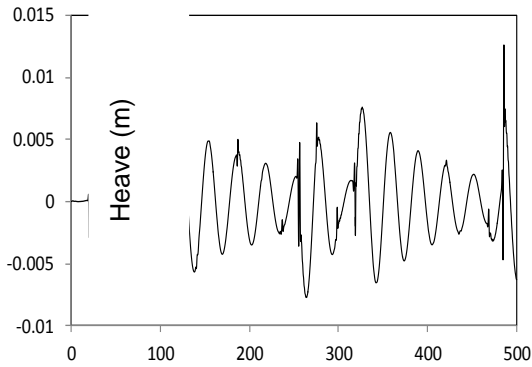


Fig.10b: Time history of heave response (30°).

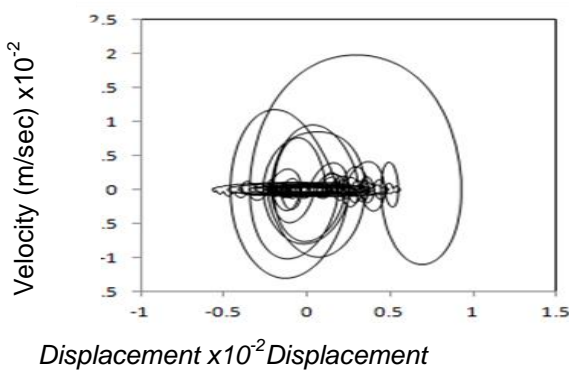


Fig. 11a: Phase plan for heave response (0°).

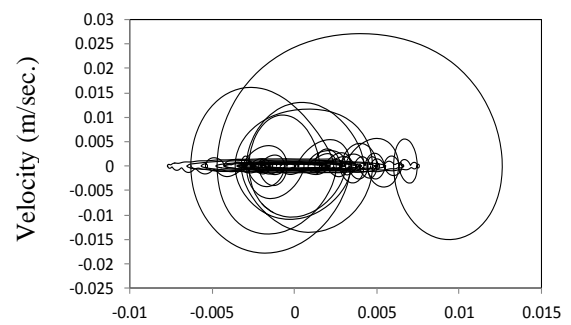


Fig.11b:Phase plan for heave response (30°).

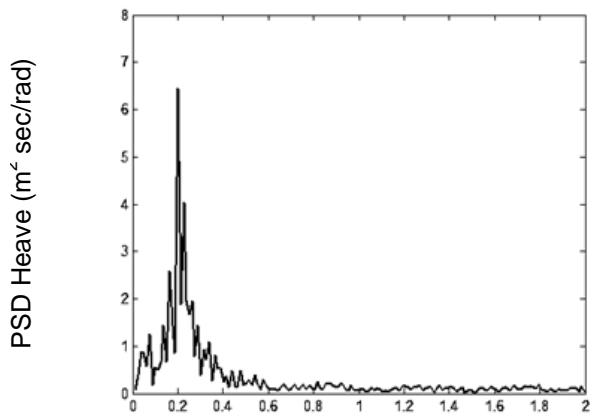


Fig. 12a: PSD of heave displacement (0°).

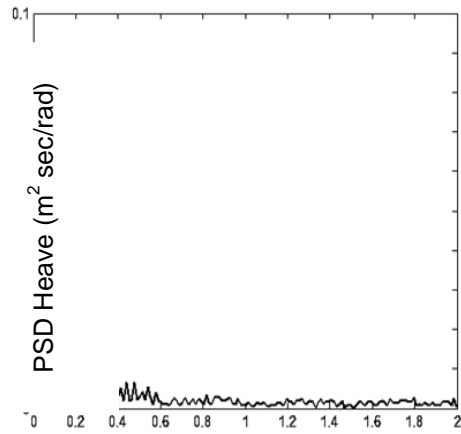


Fig.12b: PSD of heave displacement (30°).

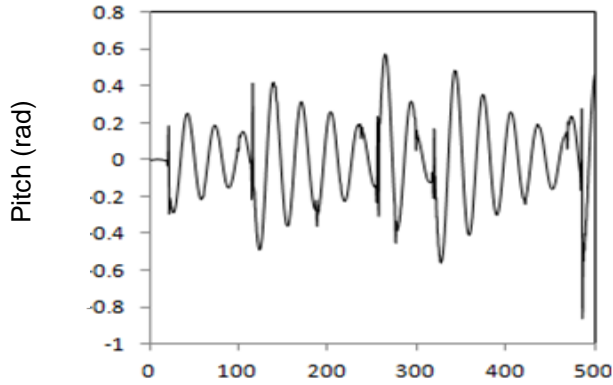


Fig. 13a: Time history of pitch response (0°).

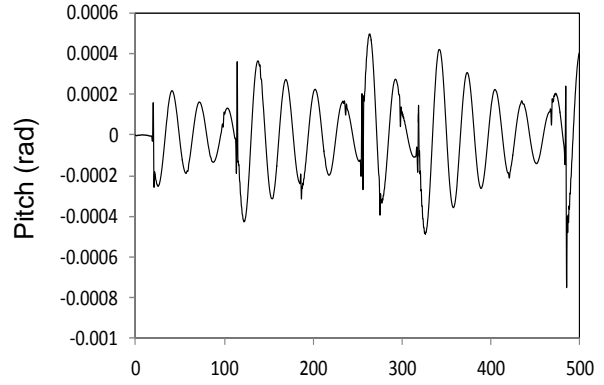


Fig.13b: Time history of pitch response (30°).

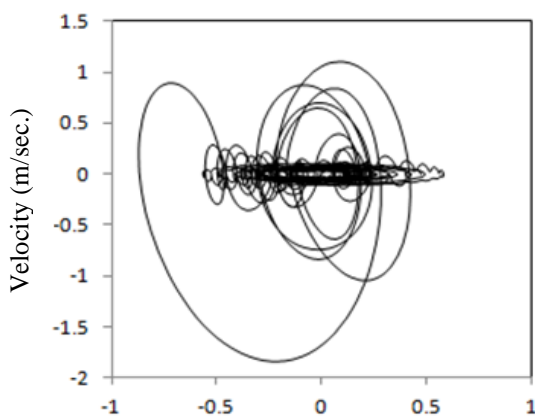


Fig. 14a: Phase plan for pitch response (0°).

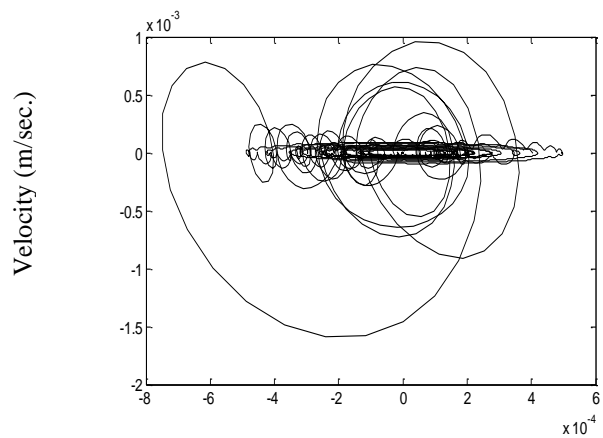


Fig.14b:Phase plan for pitch response (30°).

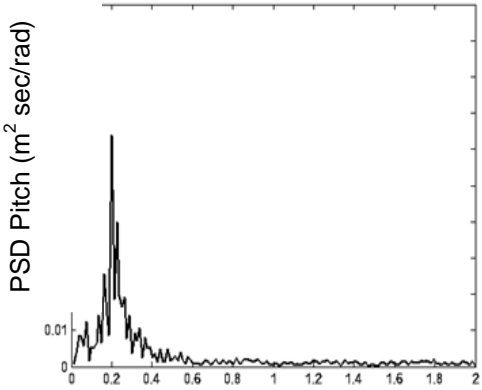


Fig. 15a: PSD of pitch displacement (0°).

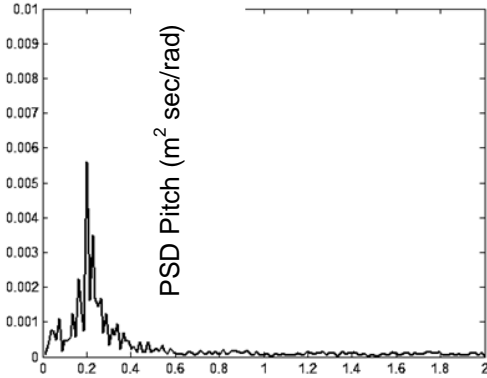


Fig.15b: PSD of pitch displacement (30°).